JOC The Journal of Organic Chemistry

Article

pubs.acs.org/joc

Spectroscopy of Protonated Tetraphenylporphyrins with Amino/Carbomethoxy Substituents: Hyperporphyrin Effects and Evidence for a Monoprotonated Porphyrin

Alexander B. Rudine, Brian D. DelFatti, and Carl C. Wamser*

Department of Chemistry, Portland State University, Portland, Oregon 97207-0751, United States

ABSTRACT: Spectrophotometric titrations for a full series of para-amino/carbomethoxy-substituted tetraphenylporphyrins were carried out using methanesulfonic acid in DMSO to study the hyperporphyrin effect across different substitution patterns. The series included zero, one, two (cis and trans), three, and four amino groups, with the remaining para substituents carbomethoxy groups. With increasing numbers of aminophenyl groups, the relative basicity increased and the hyperporphyrin effect increased, marked by a strong red band and a split Soret band. The cis diamino derivative showed a stronger hyperporphyrin effect compared to the trans isomer, which can be explained based on simple resonance forms. For the monoamino derivative, an initial increase in the Soret band upon acid titration along with well-defined isosbestic points provided evidence for a monoprotonated porphyrin, distinct from the diprotonated and triprotonated states. The relative stability of this unusual intermediate is proposed to be due to charge delocalization of the first cation to the single amino group and destabilization of the second protonation by the electron-withdrawing carbomethoxy substituents.

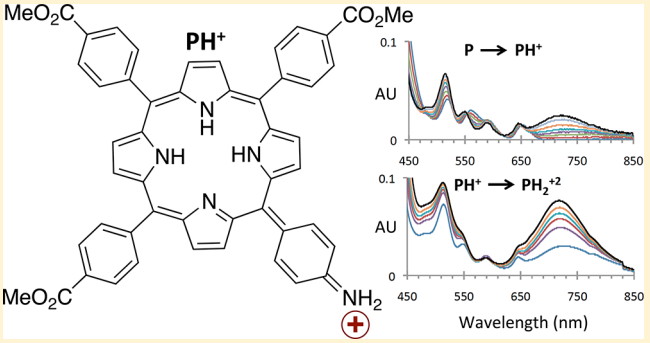

INTRODUCTION

Porphyrins and their analogs are ubiquitous in nature, being found in systems as diverse as the oxygen-binding protein hemoglobin, the oxidizing enzyme class of cytochrome P450 proteins, and the porphyrinoid molecule chlorophyll, the light absorber in photosynthesis. Porphyrins are of synthetic interest for applications such as photodynamic therapy,[1] light-emitting diodes,[2] and for use in artificial photosynthetic systems.[3,4] In each of these applications there is a great deal of interest in understanding and modulating porphyrin photophysical properties. In particular, for all the applications mentioned and more, it is of special interest to understand and enhance the red and near-infrared absorption of porphyrins.

The typical porphyrin UV−visible spectrum is characterized by a strong absorption around 400 nm (Soret band) and two (metalloporphyrin) to four (free-base porphyrin) less intense bands in the region between 450 and 700 nm (Q bands). These absorptions are well explained by the Gouterman four-orbital model, which describes the Soret and Q bands as resulting from $\pi-\pi^*$ transitions from nearly degenerate HOMOs [$a_{1u}(\pi)$ and $a_{2u}(\pi)$] and two degenerate LUMOs [$e_g(\pi^*)$].[5] Under various conditions the UV−visible spectrum of a porphyrin can show a broadened and/or split Soret band along with a greatly enhanced, red-shifted absorption beyond where the Q-bands usually end. This type of spectrum is characteristic of a hyperporphyrin, which is defined as a porphyrin that exhibits prominent extra absorption bands in the region $\lambda > 320$ nm which are not attributed to porphyrin $\pi-\pi^*$ transitions.[5] Hyperporphyrin-type spectra have been reported in metal-to-porphyrin charge transfer (CT) transitions[6] and when appropriately substituted porphyrins are subjected to acidic[7−11] or basic[12−15] conditions. Oxidation of porphyrins with electron-rich phenyl substituents also gives hyperporphyrin spectra.[16] In general, the extra absorption bands are attributed to π (substituted phenyl)$-\pi^*$ (porphyrin) CT transitions.

The protonation chemistry of the porphyrin ring has been well studied, and the macrocycle exists in acidic media in three main forms: free base (P), monocation (PH^+), and dication (PH_2^{+2}).[12,17−33] However, evidence for the monocation species has been minimal.[17,25,27−29,32,33] It has been suggested that the monocation is hard to observe because the first protonation of the porphyrin ring requires a loss of planarity that makes the second protonation even more favorable, such that little of the monoprotonated species is present at any given time.[27,32,34] In several cases, UV−visible absorption data have indicated the existence of a monoprotonated species,[22,35,36] and it has been characterized as having three absorptions in the Q-band region.[19,22,36] NMR spectroscopy has indicated the presence of a monocation in the case of a hydrocarbon-capped porphyrin.[37] The crystal structures of the octaethylporphyrin and dodecaphenylporphyrin monocations have also been presented.[34,38] In the two reported cases of tetraphenylporphyrin monocation species,[34,35] either bulky, weakly coordinating

Received: April 8, 2013
Published: May 10, 2013

 © 2013 American Chemical Society dx.doi.org/10.1021/jo400742f | J. Org. Chem. 2013, 78, 6040−6049

anions were needed to stabilize the monocation,[35] or a saddle-distorted porphyrin was generated such that the planarity of the four interior ring nitrogens is broken, thus relieving the steric destabilization of having three coplanar hydrogen atoms inside the macrocyclic ring.[34]

Hyperporphyrins derived from acidic conditions (porphyrin dications) have been studied extensively with a wide range of substrates, such as tetrakis(*p*-aminophenyl)porphyrin (**TAPP**),[11] a series of one, two (cis) and four dimethylaminophenyl/phenyl porphyrins,[8,9,39] a monoaminophenyl/tris(pentafluorophenyl)porphyrin,[40] and a series of trans disubstituted arylethynylporphyrins.[7] However, to the best of our knowledge, a study of the hyperporphyrin behavior for a full series of mixed-substituent porphyrins with both electron-donating and electron-withdrawing groups has yet to be realized.

In this study we present the hyperporphyrin spectra for a full series of para-substituted tetraphenylporphyrins (Figure 1),

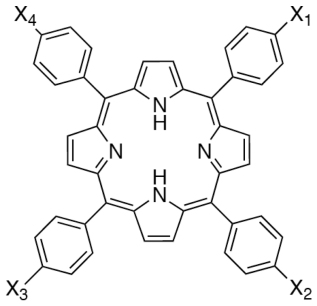

TCMPP	= $X_1, X_2, X_3, X_4 = COOCH_3$
$TACM_3PP$	= $X_1 = NH_2$, $X_2, X_3, X_4 = COOCH_3$
Trans	= $X_1, X_3 = NH_2$, $X_2, X_4 = COOCH_3$
Cis	= $X_1, X_2 = NH_2$, $X_3, X_4 = COOCH_3$
TA_3CMPP	= $X_1, X_2, X_3 = NH_2$, $X_4 = COOCH_3$
TAPP	= $X_1, X_2, X_3, X_4 = NH_2$

Figure 1. Structure of para-substituted tetraphenylporphyrins with abbreviations and substitution patterns for the amino/carbomethoxyphenylporphyrins studied.

having zero, one, two (cis and trans), three, and four electron-donating amino groups, with the other substituents being electron-withdrawing carbomethoxy groups. We will also provide spectroscopic evidence for the existence of a monoprotonated hyperporphyrin intermediate and discuss reasons for the stability of the monocation in this case.

RESULTS

Porphyrin Absorption Spectroscopy. The free-base meso-tetraarylporphyrin (P) absorption spectrum is characterized by an intense Soret band at about 400 nm and four smaller Q bands between 450 and 700 nm. Upon titration with acid to the dication (PH_2^{+2}), the absorption spectrum of most meso-tetraarylporphyrins typically show a red-shifted Soret band and a collapse from four Q bands to two, indicating an increase in symmetry from 2-fold to 4-fold. As a reference, the acid titration spectrum for **TCMPP** is shown in Figure 2. On the other hand, if the meso-tetraarylporphyrin is substituted with strong electron-donating substituents, when it is protonated to its dication a hyperporphyrin spectrum is observed.

1. $TACM_3PP \rightarrow TACM_3PPH_3^{+3}$. The spectrophotometric titration of **$TACM_3PP$** (Figure 3) shows three distinct protonation stages, which we interpret to represent formation

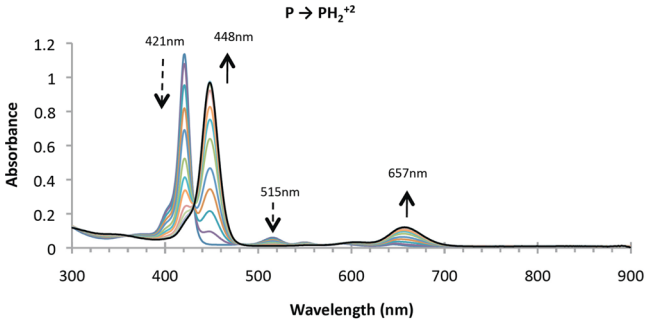

Figure 2. Spectrophotometric titration of 3 μM **TCMPP** with 0−5 mmol of MSA in DMSO. Addition of two protons gives the diprotonated porphyrin.

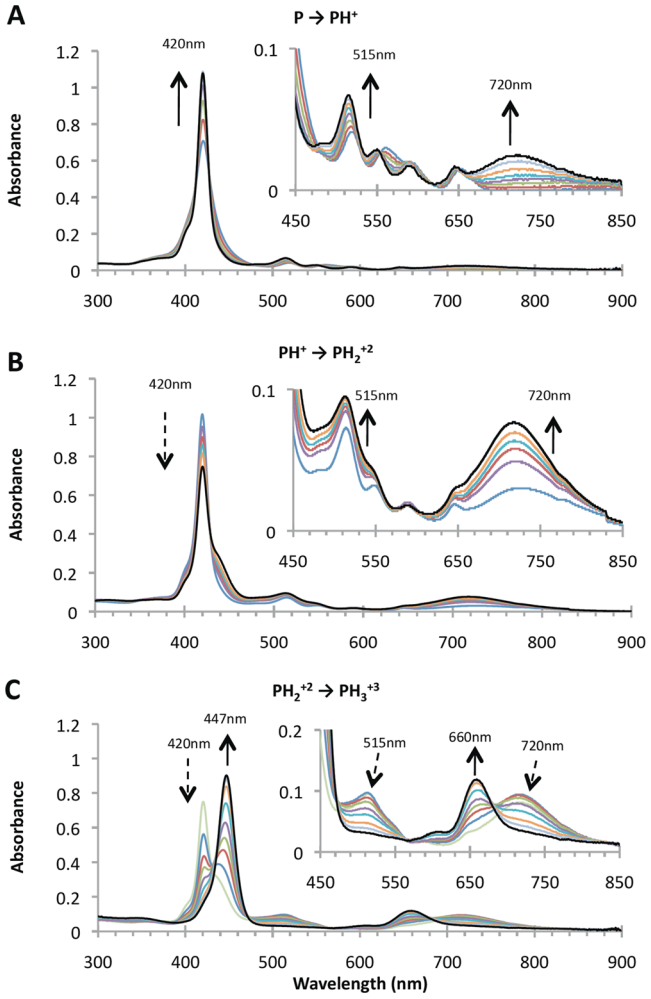

Figure 3. Spectrophotometric titration of 3 μM **$TACM_3PP$** with MSA in DMSO. (A) Addition of the first proton (0−24 μmol MSA), (B) addition of the second proton (24−150 μmol MSA), and (C) addition of the third proton to give the fully protonated porphyrin (0.15−5.0 mmol MSA).

of the monocation, dication, and trication (**A**, **B**, and **C** in Figure 3, respectively). The first phase to form the monocation shows a well-defined isosbestic point at 550 nm (inset of Figure 3A), an increase in the first Q-band at 515 nm, and a new broad hyperporphyrin absorption at 720 nm. Further evidence of a distinct transition during this initial phase is the sharpening and strengthening of the Soret absorbance at 420 nm. To the best of

dx.doi.org/10.1021/jo400742f | J. Org. Chem. 2013, 78, 6040−6049

our knowledge this is the first example of a Soret band increase in the transition from a neutral porphyrin to its hyperporphyrin form. However, this behavior has been observed in the oxidation of a neutral porphyrin to its monocation form.[36] This is the opposite of the typical changes observed as a hyperporphyrin is formed, in which the Soret band diminishes as it splits to form a new low-energy absorbance.

During the second phase of the titration (monocation to dication, Figure 3B) the Soret absorbance decreases (420 nm) and the absorbance at 515 nm continues to increase (characteristic of a hyperporphyrin split Soret absorbance), while the absorbance at 720 nm also steadily increases. The isosbestic point at 550 nm disappears. During the third phase of the titration (dication to trication, Figure 3C) the Soret band shifts from 420 to 447 nm while the split Soret absorbance at 515 nm diminishes. The hyperporphyrin band at 720 nm disappears and is replaced by an absorbance at 660 nm that is characteristic of a symmetric fully protonated porphyrin.

The acid titrations were followed spectrophotometrically at three or more distinct wavelengths to distinguish the relative concentrations of different species at different points in the titrations, using the method of Splan[7] as described in the Experimental Methods section and illustrated in Figure 4. Apparent pK_a values were obtained from the x-intercepts at which the acid concentration was sufficient to generate equal concentrations of both the acid and conjugate base forms. These are considered apparent pK_a values because of the nonaqueous solvent (DMSO) and the unidentified state of ionization of MSA. Nevertheless, they are useful indicators of the relative basicity of the different derivatives, which are tabulated in Table 2. The specific data for the three protonation stages of **TACM$_3$PP** are presented in detail in Figure 4 because of the special interest in documenting the novel monoprotonated state.

2. Trans → TransH$_4^{+4}$. The titration of the trans disubstituted derivative goes through two distinct spectroscopic stages from neutral porphyrin to dication and from dication to the fully protonated species **TransH$_4^{+4}$** (Figure 5A and B, respectively).

The original broad Soret band at 424 nm increases in intensity, sharpens, and blue shifts to 420 nm, while the hyperporphyrin bands at 500 and 760 nm continue to increase with added acid. The Soret band at 420 nm begins to decline after 0.15 mmol of MSA has been added. Once again the initial increase in the Soret band and the incomplete correlation with other hyperporphyrin bands may signal the presence of an intermediate species such as the monoprotonated porphyrin; the evidence here is less clear than in the case of **TACM$_3$PP**. During the second stage the split Soret peaks coalesce into a single peak at 446 nm and the hyperporphyrin absorbance at 760 nm decreases while the new absorbance grows in at 660 nm, characteristic of a fully protonated porphyrin.

3. Cis → CisH$_4^{+4}$. Upon acidification of the cis disubstituted derivative to form the dication species (Figure 6A), the Soret absorbance initially sharpens and blue shifts from 425 to 420 then decreases in intensity as a new weaker band appears at 487 nm. The new broad hyperporphyrin absorption is observed at 763 nm. It is interesting to note the marked difference between the **Cis** and **Trans** dication spectra. Compared to **Trans** the **Cis** hyperporphyrin has a much more prominent split (low-energy) Soret band (487 nm) and a weaker normal Soret band (428 nm). This difference makes the ratio of the split Soret absorbance (low energy absorbance: high energy absorbance)[8] for **Cis** much larger than that of **Trans** (0.55 versus 0.31,

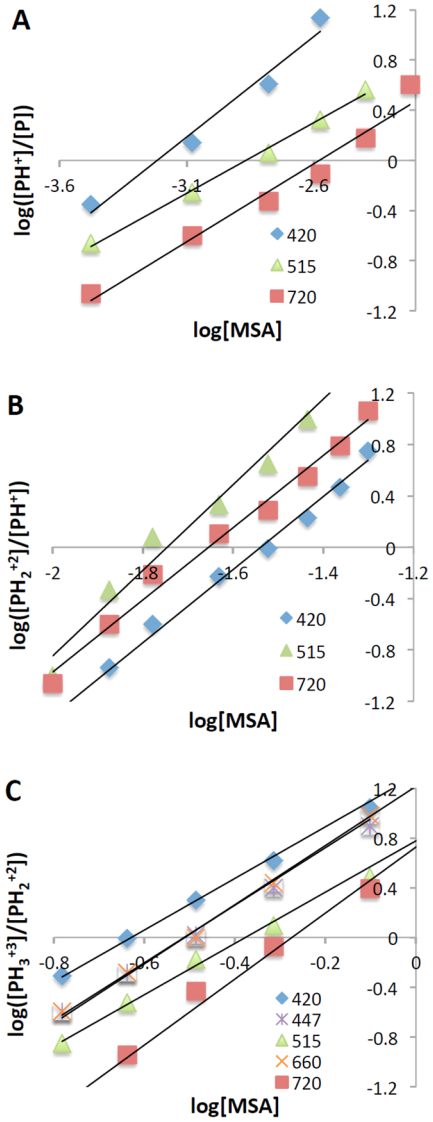

Figure 4. Log([PH$_{n+1}^{+(n+1)}$]/[PH$_n^{+n}$]) versus log [MSA] for mono, di, and triprotonated **TACM$_3$PP** (A, B, and C respectively). Data taken from the titrations shown in Figure 3A, B, and C, respectively. Apparent pK_a values are determined from the log[MSA] intercept where [PH$_{n+1}^{+(n+1)}$]/[PH$_n^{+n}$] = 1.

respectively). As the titration continues (Figure 6B, dication to fully protonated **CisH$_4^{+4}$**) the split Soret absorbance coalesces into a new Soret absorbance at 448 nm. The hyperporphyrin band at 763 nm blue shifts and decreases as the absorbance characteristic of the fully protonated porphyrin appears at 660 nm.

4. TA$_3$CMPP → TA$_3$CMPPH$_5^{+5}$. The various stages of the acid titration of **TA$_3$CMPP** are shown in Figure 7.

In the titration of **TA$_3$CMPP** to the dication (Figure 7A), the Soret band splits with the initial band steadily decreasing and blue shifting from 433 to 420 nm, with the new peak growing in at 480 nm. The ratio of the split Soret peaks is now reversed, with the higher-energy peak less intense than the lower-energy peak at 480 nm. The Q bands disappear in favor of a strong, broad hyperporphyrin absorbance at 780 nm. As the titration is continued past the dication phase to the fully protonated species (Figure 7B), the typical collapse of the split Soret band and red hyperporphyrin band is observed, with the bands characteristic

dx.doi.org/10.1021/jo400742f | J. Org. Chem. 2013, 78, 6040−6049

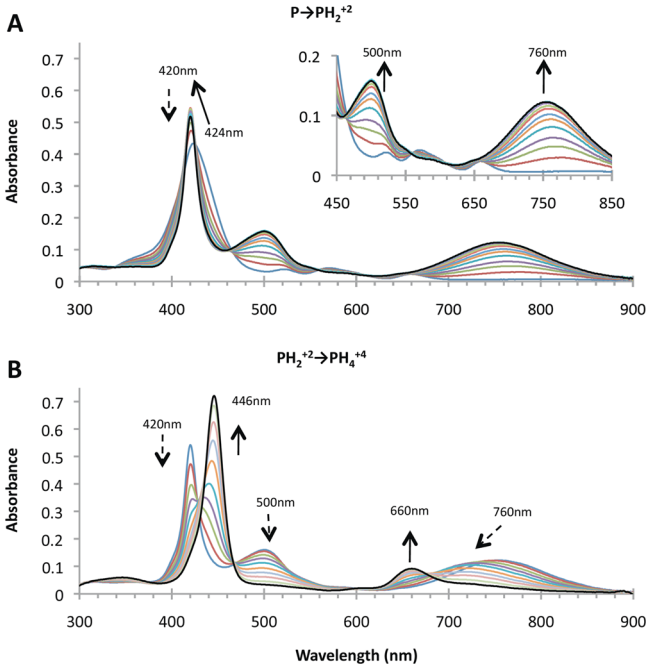

Figure 5. Spectrophotometric titration of 3 μM **Trans** with MSA in DMSO. (A) Addition of two protons to form the hyperporphyrin (0–50 μmol MSA), (B) addition of the final two protons to give the fully protonated porphyrin (0.05–8.0 mmol MSA).

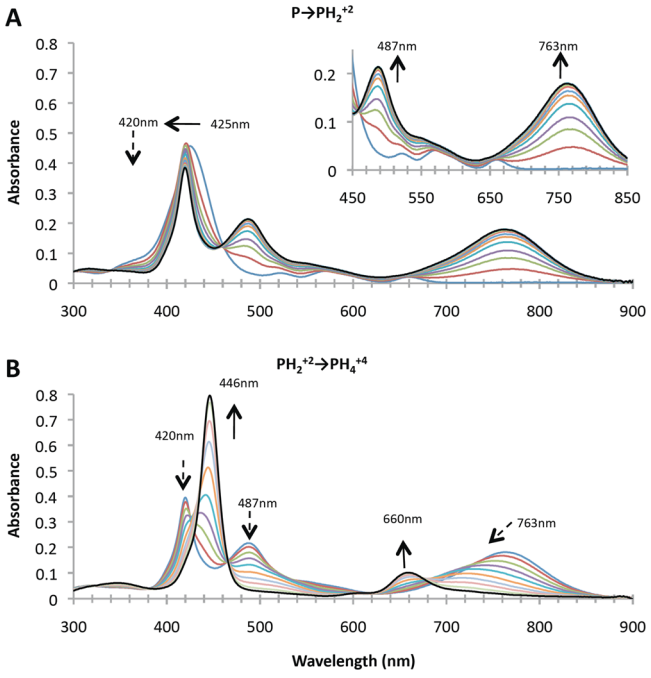

Figure 6. Spectrophotometric titration of 3 μM **Cis** with MSA in DMSO. (A) Addition of two protons to form the hyperporphyrin (0–50 μmol MSA), (B) addition of the final two protons to give the fully protonated porphyrin (0.05–8.0 mmol MSA).

of the fully protonated porphyrin appearing at 445 and 665 nm. It was not possible to distinguish protonation stages between the +2 and +5 states.

5. TAPP → TAPPH$_4^{+6}$. The spectrophotometric titration of **TAPP** has been carried out in this lab and the absorption spectra can be found elsewhere,[11] but a brief summary is presented here for comparison purposes. At the dication stage the Soret

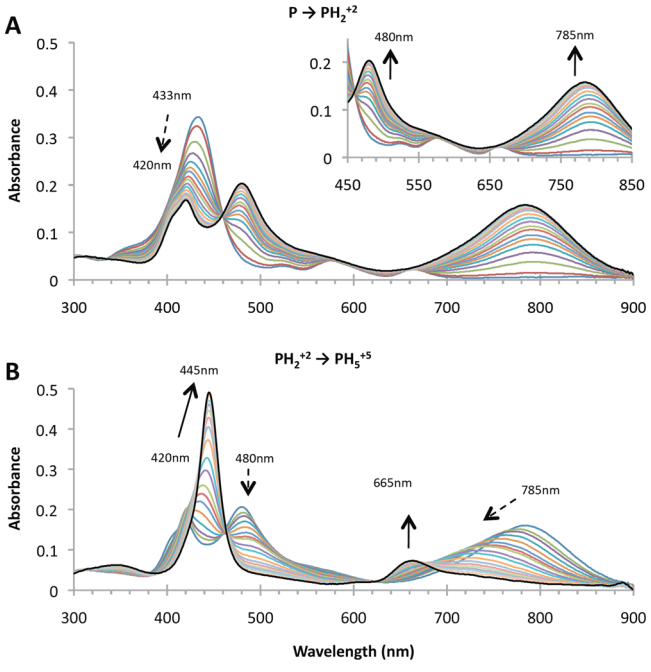

Figure 7. Spectrophotometric titration of 3 μM **TA$_3$CMPP** with MSA in DMSO. (A) Addition of two protons to form the hyperporphyrin (0–25 μmol MSA), (B) addition of the final three protons to give the fully protonated porphyrin (0.025–12.0 mmol MSA).

absorbance splits to a relatively weak absorbance at 392 nm and a broad, strong absorbance at 466 nm. The hyperporphyrin absorbance is very strong, centered at 811 nm and covering over 200 nm. Upon adding the third through sixth protons, the spectrum gradually reverts to a typical symmetric fully protonated porphyrin spectrum with a Soret band at 443 nm and a Q-band absorbance at 660 nm.

Absorbance peak positions and extinction coefficients for the free base (**P**) and cationic (**PH$^+$**, **PH$_2^{+2}$**, and **PH$_{n+2}^{+n+2}$**) forms of all six derivatives studied are listed in Table 1.

Relative Basicities. The molar concentrations of MSA required to reach the half-equivalence point and apparent pK_a values for each stage (**PH$^+$**, **PH$_2^{+2}$**, and **PH$_{n+2}^{+n+2}$**) are listed in Table 2.

DISCUSSION

The acid titrations for this full series of amino/carbomethoxyphenyl porphyrins illustrate clear trends in the series from monoamino to trans-diamino to cis-diamino to triamino to tetraamino. The trends are consistently in the same order in terms of relative basicities, the wavelength and intensity of the new broad red peak (hyperporphyrin band), and the wavelength and intensity of the new split Soret band (Figures 3–7 and Tables 1–2). In every case, the trends may be explained by the generation of a diprotonated porphyrin with increasing opportunities for conjugation between the peripheral aminophenyl substituents and the porphyrin core (a hyperporphyrin). For each trend the driving force is a greater ability to donate electron density from the peripheral amino groups to the porphyrin core, increasing with the number of electron-donating aminophenyl substituents. However, the disubstituted isomers show that the cis derivative has stronger hyperporphyrin effects than the trans derivative, indicating that molecular geometry is also important (via resonance forms) in determining the extent of the hyperporphyrin effect.

dx.doi.org/10.1021/jo400742f | J. Org. Chem. 2013, 78, 6040–6049

Table 1. Porphyrin Peak Absorbance Wavelengths and Extinction Coefficient Values

	λ_{max} (nm) (ε, × 10^3 M^{-1} cm^{-1})			
porphyrin	P	PH^{+1}	PH_2^{+2}	PH_{n+2}^{+n+2}
TCMPP	421 (*380*)			
	515 (*20*)			448 (*360*)
	550 (*11*)			657 (*45*)
	590 (*8*)			
	645 (*7*)			
$TACM_3PP$		420 (*360*)		
	421 (*240*)	550 (*10*)	420 (*230*)	
	519 (*14*)	515 (*22*)	513 (*32*)	447 (*330*)
	560 (*10*)	589 (*6*)	716 (*26*)	659 (*44*)
	653 (*5*)	645 (*6*)		
		720 (*8*)		
Trans	423 (*140*)		420 (*170*)	446 (*280*)
	521 (*13*)		500 (*53*)	660 (*36*)
	570 (*14*)		756 (*41*)	
	660 (*8*)			
Cis	425 (*150*)		420 (*130*)	446 (*310*)
	522 (*11*)		487 (*71*)	660 (*39*)
	571 (*14*)		763 (*60*)	
	660 (*7*)			
TA_3CMPP	433 (*110*)		420 (*56*)	445 (*200*)
	523 (*10*)		480 (*68*)	664 (*30*)
	576 (*14*)		784 (*53*)	
	663 (*7*)			
TAPP[a]	438 (*160*)		392 (*40*)	443 (*220*)
	528 (*10*)		466 (*92*)	660 (*31*)
	579 (*20*)		811 (*70*)	
	669 (*10*)			

[a]TAPP data from previous work.[11]

Table 2. Concentrations of MSA (mM) Required to Reach Approximate Half-equivalence Points and Apparent pK_a Values (p$K_{a,app}$)[a]

	[MSA] (mM), p$K_{a,app}$					
porphyrin[b]	P → PH^+		P → PH_2^{+2}		PH_2^{+2} → PH_{n+2}^{+n+2}	
TCMPP					150	0.8
$TACM_3PP$	1.3	2.9	23	1.6	350	0.5
Trans			0.8	3.1	290	0.5
Cis			0.7	3.1	290	0.5
TA_3CMPP			0.2	3.8	300	0.5
TAPP[c]			0.01	5	290	0.5

[a]p$K_{a,app}$ = −log[MSA]$_{1/2\ eq\ pt.}$ [b]3 mL of a 3.0 μM solution [c]3 mL of a 6.0 μM solution - data from previous work.[11]

Relative basicities are determined by the amount of acid titrant needed to reach half-equivalence points. Optical and NMR studies have confirmed that the initial protonation in aminophenyl-substituted porphyrins is on the pyrrole nitrogens within the porphyrin core, rather than on the peripheral amino groups.[8,9,40] Each amino substituent (replacing an electron-withdrawing carbomethoxy substituent) increases the relative basicity of the pyrrole nitrogens, indicted by the significant decrease in acid required to generate the hyperporphyrin (PH_2^{+2}) as the number of amino substituents increase. This effect is readily explained by the availability of resonance forms that delocalize the positive charge of the conjugate acid to the peripheral amino groups. Upon addition of excess acid, complete protonation converts the amino groups to ammonium ions, and spectra of the fully protonated porphyrins appear as expected for tetraphenylporphyrins with noninteracting substituents (i.e., like diprotonated **TCMPP**, Figure 2). Interestingly, the amount of acid required to continue the protonation of the hyperporphyrins is approximately equivalent throughout the whole series; about 300 mM MSA is required for full protonation, regardless of whether the final protonation state is +3 or +6.

The red hyperporphyrin band appears farther into the red and increases in breadth and intensity as the number of amino groups increases, with peak wavelengths moving from 716 to 811 nm (Figure 8). **TA_3CMPP** does not follow the increasing

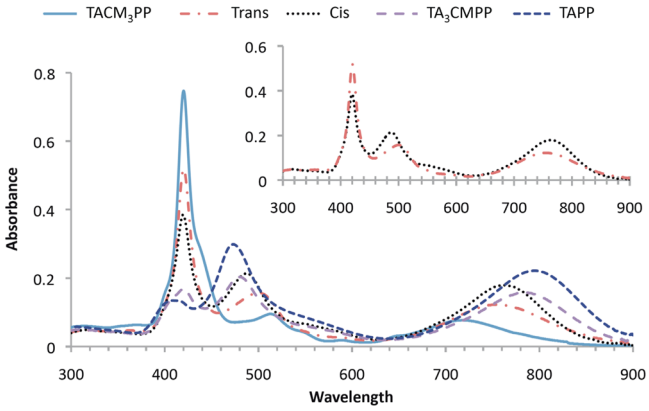

Figure 8. Comparison of the diprotonated hyperporphyrin spectra for the amino/carbomethoxyphenylporphyrin series with one to four aminophenyl substituents. (Inset) Comparison of the dication spectra for the cis and trans diaminophenyl derivatives.

intensity pattern seen in the other four cases; we believe this may be due to a concentration lower than calculated brought on by sample degradation. However in every other metric the trends are consistent. The red hyperporphyrin peak has been assigned as a charge-transfer transition from an aminophenyl group to a porphyrin π^* LUMO.[41,42] With more aminophenyl groups available, the transition is distinctly stronger and moves to lower energy (longer wavelength).

Earlier we examined substituent effects on hyperporphyrin spectra using Hammett correlations and found that the position and intensity of the long-wavelength absorption peak can be correlated with the Hammett sigma constant; although any electron-donating substituent can give rise to a detectable hyperporphyrin effect, it is the strong electron donors such as amino or alkoxy that give the obvious examples.[11,43] For example, a cis-dimethylaminophenylporphyrin was studied by Ojadi et al.,[8] showing a strong hyperporphyrin spectrum comparable to our cis-diaminophenylporphyrin. The Ojadi study did not examine trans or trisubstituted cases, but did study a monosubstituted dimethylaminophenylporphyrin without identifying a monoprotonated form of the porphyrin.[8] In this case, the range of acidities used appears to have stepped over the range that would have been necessary to see the initial monoprotonation.

Splan and co-workers[7] recently reported a series of trans disubstituted porphyrins comparing the effects of substitution on phenylethynyl groups to those on phenyl groups. The phenylethynyl linker was clearly more effective at transmitting the strong electron-donating capability of *p*-dimethylamino groups to a protonated porphyrin, with a stronger and longer

dx.doi.org/10.1021/jo400742f | J. Org. Chem. 2013, 78, 6040−6049

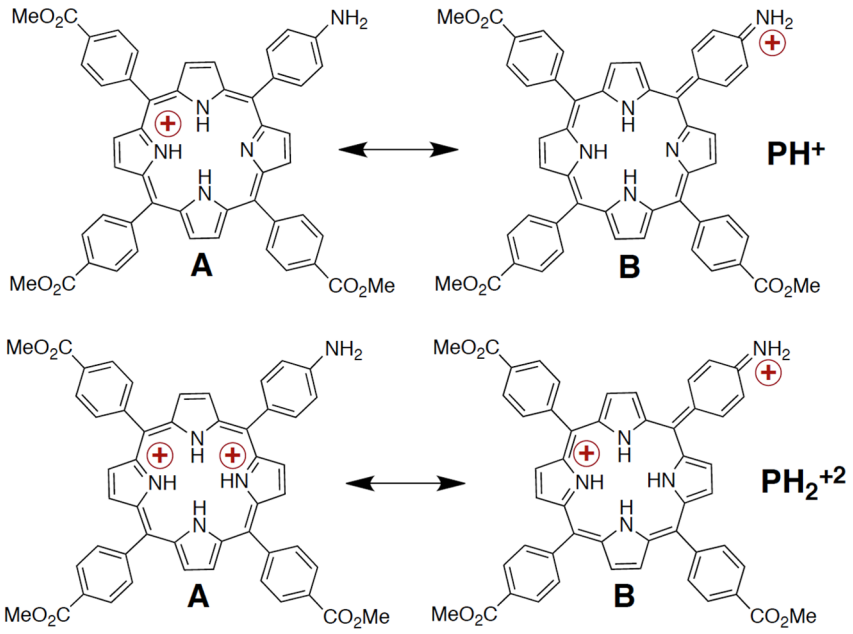

Figure 9. Selected resonance forms for **TACM$_3$PP** for addition of the first proton (top) and the second proton (bottom), illustrating the sites for delocalization of the positive charge. Type **A** and **B** forms are discussed in the text.

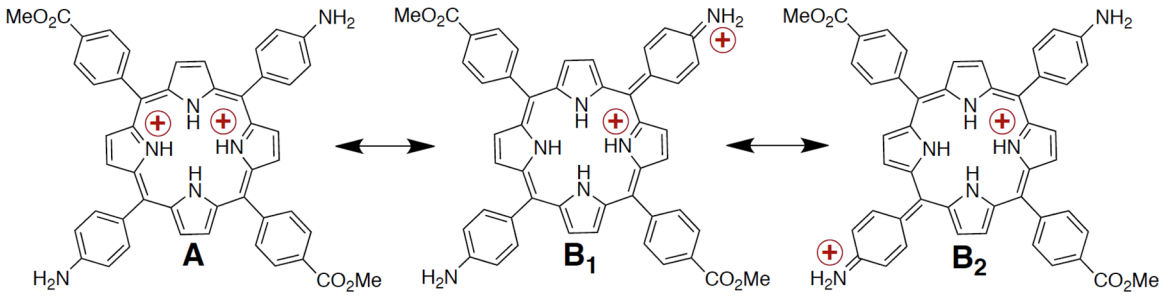

Figure 10. Selected resonance forms for diprotonated **Trans**, illustrating the sites for delocalization of the positive charge. Both charges cannot be placed on the trans-diamino groups simultaneously. Type **A** and **B** forms are discussed in the text.

wavelength red band than the corresponding trans-disubstituted phenylporphyrin. This effect is attributed to the difficulty in achieving coplanarity between the phenyl and porphyrin rings, which is relieved when the alkynyl spacer is used. The coplanarity that is achievable with the alkynyl spacer is clearly more important than the greater distance in transmitting the favorable effects of conjugation.

The Soret band split also becomes more pronounced with greater numbers of aminophenyl substituents. As the number of aminophenyl substituents increase, the low-energy component of the transition becomes increasingly stronger at the expense of the high-energy component, and it also significantly shifts to the blue (Figure 7). Examining the relative intensity of the high-energy to the low-energy component of the split Soret band, we observe in order of increasing aminophenyl substituents intensity ratios as follows: 0.14, 0.31, 0.55, 1.21, and 2.3 (for **TACM$_3$PP**, **Trans**, **Cis**, **TA$_3$CMPP**, and **TAPP**, respectively). Roughly there is a doubling that occurs with each step of increased favorability of a hyperporphyrin charge delocalization.

This trend holds with literature comparisons as well. Comparing reported work on *p*-dimethylamino derivatives, the trans derivative gives a Soret ratio of about 0.6 (based on the extinction coefficients reported)[7] and the cis derivative gives a ratio of about 1.[8] It is also notable that the split Soret ratio for the trans-bis[(4-dimethylamino)phenylethynyl]porphyrin derivative reported by Splan and co-workers shows a split ratio Soret of 0.31,[7] on par with what we report here for **Trans**.

The intensity of the red hyperporphyrin band relative to the blue Soret band mirrors the relationship of the split Soret bands. An approximate doubling of the ratio is seen for every step by which hyperporphyrin formation favorability increases, as summarized in Table 3.

Resonance effects can be used to correlate most of the observed trends for this series. As would be expected, increasing the number of amino substituents increases the total number of available resonance forms. However, beyond the number of amino substituents, there are geometric effects that significantly influence the number and types of resonance forms that can be drawn for the different cases. For **TACM$_3$PP** (Figure 9) and **Trans** (Figure 10), none of the resonance forms written can support delocalization of both positive charges from the interior pyrrole nitrogens to the aminophenyl substituents. For the former it is a purely statistical effect, that is, only one good donor group is available to delocalize the positive charge. In **Trans**, however, there are two donor groups but the arrangement of the π system does not allow for both charges to be delocalized at the same time. For **Cis** (Figure 11) the arrangement of the donor groups is such that delocalization of both charges can occur. For **TA$_3$CMPP** (Figure 12), there are two pairs of cis donor groups that can similarly delocalize both charges. **TAPP** (resonance

dx.doi.org/10.1021/jo400742f | J. Org. Chem. 2013, 78, 6040−6049

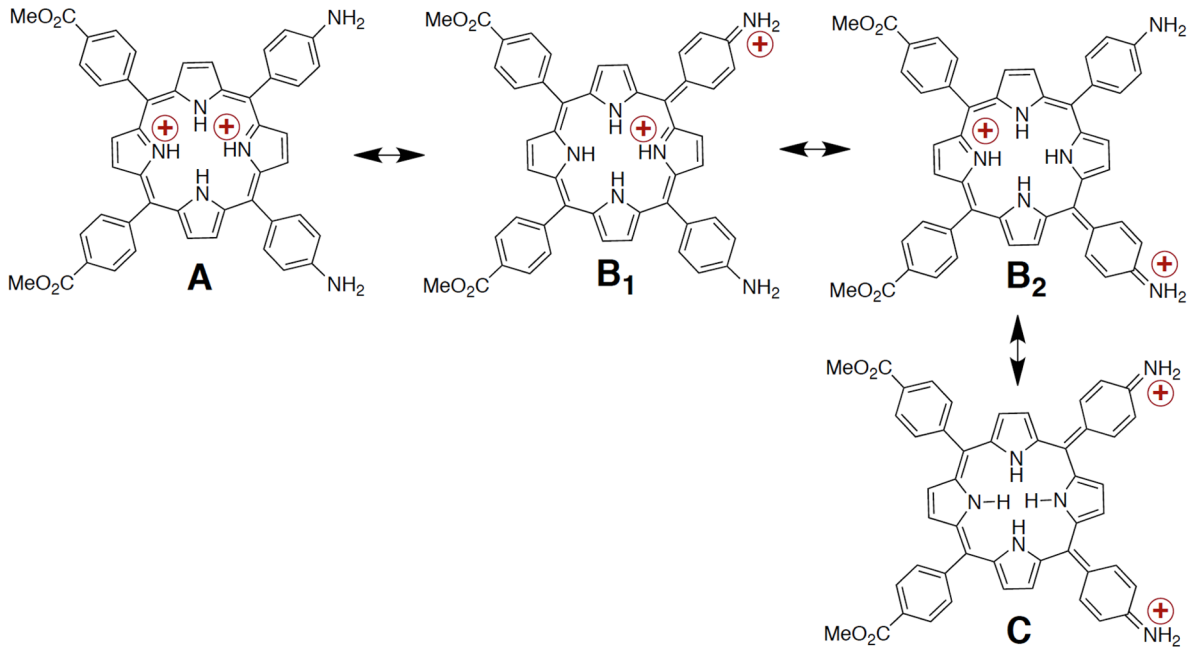

Figure 11. Selected resonance forms for diprotonated **Cis**, illustrating the sites for delocalization of the positive charge. Note that both charges can be placed on the cis-diamino groups simultaneously. Type **A**, **B**, and **C** forms are discussed in the text.

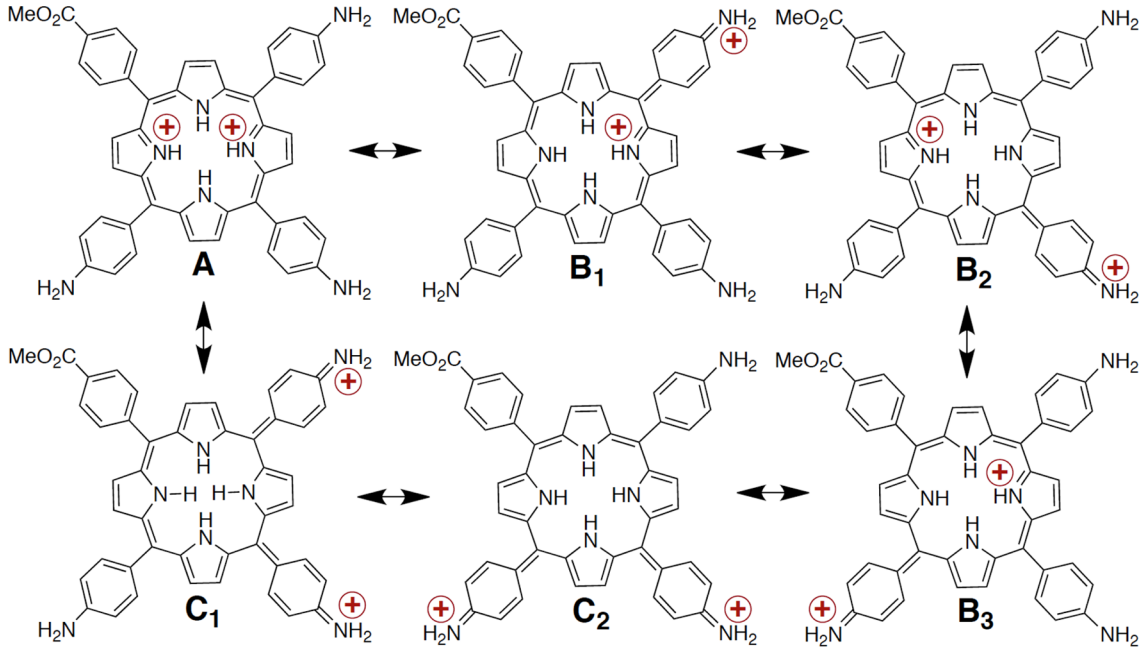

Figure 12. Selected resonance forms for diprotonated **TA_3CMPP**, illustrating the sites for delocalization of the positive charge. Note that both charges can be placed on cis-diamino groups simultaneously. Type **A**, **B**, and **C** forms are discussed in the text.

structures not shown) has four amino substituents and four unique cis orientations that can delocalize both positive charges. The increase in the number of resonance forms, especially those forms that delocalize both charges, manifests itself as a stronger hyperporphyrin effect and gives rise to all the trends discussed previously.

Hyperporphyrin Resonance Forms. The spectroscopy of porphyrins has long been understood in the framework presented by Gouterman.[44] He has also presented an organizational framework for specific cases of anomalous spectroscopy such as hyperporphyrins.[8] Basically, **A** type spectra are normal porphyrin spectra, in which the four meso substituents do not interact significantly with the porphyrin ring; there are both neutral and diprotonated **A** type spectra, as illustrated in Figure 2 where all substituents are carbomethoxy. When meso substituents are capable of strong interaction with the porphyrin π system, however, the chromophore can be extended significantly beyond the porphyrin core and anomalous spectra result. In a type **B** spectrum, one such substituent interacts, while in a type **C** spectrum, two such substituents interact. Careful manipulation of the available resonance forms show that for diprotonated porphyrins (where the two protons are added at the central nitrogens), delocalization requires that donor groups be available at cis meso positions, leading to the **C** type

dx.doi.org/10.1021/jo400742f | J. Org. Chem. 2013, 78, 6040−6049

resonance forms shown in Figures 11 and 12. The trans orientation does not allow for a **C** type resonance form. Continued protonation leads all of our porphyrins back to a type **A** spectrum, in which all meso substituents are noninteracting, that is, either carbomethoxy groups or ammonium ions.

Table 3 summarizes the effects of increasing numbers of the different resonance forms available on what we call the hyperporphyrin effect, that is, a stronger and more red-shifted hyperporphyrin band (H) and a split Soret band with increasing strength at the longer-wavelength component (S2/S1). The numbers of resonance forms of each type cited in Table 3 are not the total number of resonance forms possible (which would be very numerous), rather they represent the number of unique peripheral positions to which the positive charges may be delocalized.

Table 3. Porphyrin Peak Absorbance Wavelengths (Soret S1 and S2 and Hyperporphyrin H Bands) with Extinction Coefficient Values, Correlated with Resonance Forms Available

	PH_2^{+2}				
porphyrin	λ_{max} (nm) (ε, $\times 10^3$ M^{-1} cm^{-1})	ε(S2):ε(S1)[a]	ε(H):ε(S1)[b]	Type B forms	Type C forms
$TACM_3PP$	420 (*230*)	0.14	0.11	1	0
	513 (*32*)				
	716 (*26*)				
Trans	420 (*170*)	0.31	0.24	2	0
	500 (*53*)				
	756 (*41*)				
Cis	420 (*130*)	0.55	0.46	2	1
	487 (*71*)				
	763 (*60*)				
TA_3CMPP	420 (*56*)	1.21	0.95	3	2
	480 (*68*)				
	784 (*53*)				
TAPP[e]	392 (*40*)	2.3	1.75	4	4
	466 (*92*)				
	811 (*70*)				

[a]Split Soret intensity ratio.[8] [b]Hyperporphyrin: Soret S1 intensity ratio. [e]TAPP data from previous work.[11]

Evidence for a Monoprotonated Porphyrin. Evidence for the elusive monoprotonated porphyrin is scant in the literature.[27−29] Formation of the monocation is proposed to cause significant deformation of the porphyrin ring in order to counteract the steric destabilization of having three protons confined to the interior of the macrocycle.[27,32,34] However, reports of monocation porphyrins have appeared; in these cases, various means for stabilization of a single protonation have allowed their observation and characterization.[34,35] In this study, careful observation of the early stages of the spectrophotometric acid titration of **$TACM_3PP$** indicate a significant absorbance increase in the Soret band (from about 0.7 to 1.1 AU), as well as a well-defined isosbestic point at 550 nm as a distinct initial phase of the titration (up until 25 μmoles of MSA added). After the Soret band reached its maximum absorbance of 1.1 (at 420 nm), its intensity began to decrease and the isosbestic point at 550 nm disappeared. As the Soret band diminished, other typical signs of dication formation became more pronounced; the hyperporphyrin band (about 720 nm) increased and the low-energy absorbance of the split Soret band (515 nm) became more intense as the original Q bands continued to disappear. The observation of two distinct phases during the initial titration is taken as evidence that the monoprotonated porphyrin can be the majority species early in the titration. The driving force in this case is proposed to be resonance stabilization of the first protonation by electron donation from the lone amino group to the porphyrin core, creating a unique thermodynamic favorability for the first protonation. With only one amino group available, generation of the dication on the subsequent protonation step does not generate any further stabilization to the system. In fact with electron-withdrawing carbomethoxy groups on the three remaining phenyl rings, resonance destabilization should decrease the favorability of the second protonation. Thus, three factors may be instrumental in stabilizing the monocation intermediate of **$TACM_3PP$**: (1) effective charge delocalization of the first positive charge to the single amino substituent, (2) unavailability of comparable charge delocalization for the second positive charge, and (3) relative destabilization of subsequent positive charges by the three carbomethoxyphenyl groups.

The **Trans** derivative shows characteristics intermediate between **$TACM_3PP$** and **Cis**, consistent with resonance forms that do not allow the ability to delocalize both positive charges to the two trans aminophenyl groups. It is also possible to observe subtle evidence for the monoprotonated species in the **Trans** spectrophotometric acid titration. In this case, possible evidence for the monocation is a small initial increase in the Soret absorbance for **Trans**, analogous to the increase in the Soret band for **$TACM_3PP$**. This initial increase of the Soret band is smaller than that observed for **$TACM_3PP$** (0.12 versus 0.38 absorbance units), and it is not possible to detect isosbestic points or stable spectra between protonation steps, suggesting that the monocation in this case is much less abundant. This is understandable for **Trans**, for which diprotonation becomes significantly more favorable than it would be for **$TACM_3PP$**. Even though both charges are unable to delocalize to the two trans amino groups simultaneously, the charges can be delocalized to each of the two trans amino groups independently. In **$TACM_3PP$**, the second charge must remain localized in the porphyrin core.

■ CONCLUSIONS

Acid titrations of aminophenyl-substituted porphyrins show that the positive charges generated upon protonation can be effectively delocalized to the aminophenyl groups. Such delocalization shows distinctive spectra characteristic of hyperporphyrins, with a strong absorption in the far red as well as a split Soret band. Hyperporphyrin spectra are described as resulting from structures in which there is increased planarity and conjugation between the peripheral aryl groups and the porphyrin core. The extent of the hyperporphyrin effect increases with the number of aminophenyl groups, and cis is distinctly more effective than trans, which is consistent with the resonance forms available. Detection of the relatively rare monoprotonated porphyrin was observed in the case of the monoamino derivative at early stages of the acid titration.

■ EXPERIMENTAL METHODS

Materials. Solvents and reagents were the highest commercial grade and used as received. DMSO (spectrophotometric grade) was from Sigma-Aldrich. Methanesulfonic acid (MSA) (99% extra pure) was from Acros Organics. Tetrakis(4-carboxyphenyl)porphyrin (**TCPP**)

dx.doi.org/10.1021/jo400742f | J. Org. Chem. 2013, 78, 6040−6049

and **TAPP** were from Frontier Scientific. **TCMPP** was synthesized using the Adler-Longo method.[45]

Synthesis. General synthetic procedures for the mixed-substituent (4-amino/carbomethoxyphenyl)porphyrins (**TA_xCM_yPP**, Figure 1).[46] A solution of **TCPP** and polyphosphoric acid was warmed to 100°. To this, 2 equiv of $NH_2OH{\bullet}HCl$ was added and the mixture was slowly heated to 160° over 3 h. Upon cooling to room temperature, a solution of conc. H_2SO_4 and CH_3OH (1:10) was slowly added and the resulting mixture was heated at reflux for 36 h. The reaction mixture was neutralized with concentrated NH_4OH to a pH of 5.5. The dark solution was extracted with chloroform, washed with water, and dried over Na_2SO_4. The solution was evaporated to dryness and dried in vacuo overnight affording a dark purple solid. Isolation via column chromatography (silica gel 230−400 mesh), eluting with 4:1 CH_2Cl_2/ethyl acetate and 1% triethylamine, yielded **TCMPP**, **$TACM_3PP$**, **Trans**, **Cis**, **TA_3CMPP**, and **TAPP** as six purple bands in that order.[46]

Spectroscopy. Typical UV−visible spectroscopy was performed from 300 to 900 nm using a single visible light source and single detector setting. Sample speed was medium with sample interval of 0.2 nm and a slit width corresponding to 3 nm.

Titrations. Porphyrin titrations were carried out by adding diluted (DMSO) or pure MSA in 2−5 μL increments with a micropipet (2−20 μL) to a 3 μM porphyrin solution in DMSO in a 3 mL cuvette. At each addition, the resulting solution was mixed with a disposable glass pipet and the UV−visible spectrum was recorded. For later stages, samples starting with appropriate amounts of acid were prepared to minimize overall changes to the volume of the solution when pushing the porphyrin to multiple protonation levels. Typical volume changes through the diprotonated stage were ≤1% and as such were considered negligible. Beyond the diprotonation stage typical volume changes were as high as 10% and corrections were made in calculations based on these spectra. Apparent pK_a values were determined by monitoring the spectra during the titrations, using three to five characteristic wavelengths to calculate relative amounts of the species present, according to the method outlined by Splan and co-workers,[7] and illustrated in Figure 4.

AUTHOR INFORMATION

Corresponding Author

*E-mail: wamserc@pdx.edu.

Notes

The authors declare no competing financial interest.

ACKNOWLEDGMENTS

A.B.R. is grateful for support by an award from the U.S. Department of Energy Office of Science Graduate Fellowship Program (DOE SCGF). The DOE SCGF Program was made possible in part by the American Recovery and Reinvestment Act of 2009. The DOE SCGF program is administered by the Oak Ridge Institute for Science and Education for the DOE. ORISE is managed by Oak Ridge Associated Universities (ORAU) under DOE contract number DE-AC05-06OR23100. All opinions expressed in this paper are the authors' and do not necessarily reflect the policies and views of DOE, ORAU, or ORISE. B.D.D. is grateful for support from the Partners in Science Program sponsored by the M. J. Murdock Charitable Trust. Support from the Oregon Nanoscience and Microtechnologies Institute (ONAMI) and the National Science Foundation (Grant CHE-0911186) is gratefully acknowledged.

REFERENCES

(1) Sharman, W. M.; van Lier, J. E.; Allen, C. M. *Adv. Drug Delivery Rev.* **2004**, *56*, 53.

(2) Kalyani, N. T.; Dhoble, S. J. *Renew. Sust. Energy Rev.* **2012**, *16*, 2696.

(3) Walter, M. G.; Rudine, A. B.; Wamser, C. C. *J. Porphyrins Phthalocyanines* **2010**, *14*, 759.

(4) Imahori, H.; Kurotobi, K.; Walter, M. G.; Rudine, A. B.; Wamser, C. C. In *Handbook of Porphyrin Science*; Kadish, K. M., Smith, K. M., Guilard, R., Eds.; World Scientific: Singapore, 2012; Vol. *18*, p 58.

(5) Gouterman, M. In *The Porphyrins*; Dolphin, D., Ed.; Academic Press: New York, 1978; Vol. *3*, p 1.

(6) Sayer, P.; Gouterman, M.; Connell, C. R. *Acc. Chem. Res.* **1982**, *15*, 73.

(7) Goldberg, P. K.; Pundsack, T. J.; Splan, K. E. *J. Phys. Chem. A* **2011**, *115*, 10452.

(8) Ojadi, E. C. A.; Linschitz, H.; Gouterman, M.; Walter, R. I.; Lindsey, J. S.; Wagner, R. W.; Droupadi, P. R.; Wang, W. *J. Phys. Chem.* **1993**, *97*, 13192.

(9) Walter, R. I.; Ojadi, E. C. A.; Linschitz, H. *J. Phys. Chem.* **1993**, *97*, 13308.

(10) Wasbotten, I. H.; Conradie, J.; Ghosh, A. *J. Phys. Chem. B* **2003**, *107*, 3613.

(11) Weinkauf, J. R.; Cooper, S. W.; Schweiger, A.; Wamser, C. C. *J. Phys. Chem. A* **2002**, *107*, 3486.

(12) De Luca, G.; Romeo, A.; Scolaro, L. M. *J. Phys. Chem. B* **2006**, *110*, 14135.

(13) Guo, H.; Jiang, J.; Shi, Y.; Wang, Y.; Dong, S. *Spectrochim. Acta, Part A* **2007**, *67*, 166.

(14) Guo, H.; Jiang, J.; Shi, Y.; Wang, Y.; Liu, J.; Dong, S. *J. Phys. Chem. B* **2004**, *108*, 10185.

(15) Guo, H.; Jiang, J.; Shi, Y.; Wang, Y.; Wang, Y.; Dong, S. *J. Phys. Chem. B* **2006**, *110*, 587.

(16) Walter, M. G.; Wamser, C. C. *J. Phys. Chem. C.* **2010**, *114*, 7563.

(17) Abraham, R. J.; Hawkes, G. E.; Smith, K. M. *Tetrahedron Lett.* **1974**, 71.

(18) Aronoff, S. *J. Phys. Chem.* **1958**, *62*, 428.

(19) Austin, E.; Gouterman, M. *Bioinorg. Chem.* **1978**, *9*, 281.

(20) Chauvin, B.; Kasselouri, A.; Chaminade, P.; Quiameso, R.; Nicolis, I.; Maillard, P.; Prognon, P. *Anal. Chim. Acta* **2011**, *705*, 306.

(21) Cheng, B.; Munro, O. Q.; Marques, H. M.; Scheidt, W. R. *J. Am. Chem. Soc.* **1997**, *119*, 10732.

(22) Corwin, A. H.; Chivvis, A. B.; Poor, R. W.; Whitten, D. G.; Baker, E. W. *J. Am. Chem. Soc.* **1968**, *90*, 6577.

(23) De Luca, G.; Romeo, A.; Scolaro, L. M. *J. Phys. Chem. B* **2005**, *109*, 7149.

(24) De Luca, G.; Romeo, A.; Scolaro, L. M. *J. Phys. Chem. B* **2006**, *110*, 7309.

(25) Fleischer, E. B.; Webb, L. E. *J. Phys. Chem.* **1963**, *67*, 1131.

(26) Freeman, K. A.; Hibbert, F.; Hunte, K. P. P. *J. Chem. Soc., Perkin Trans. 2* **1979**, 1237.

(27) Hambright, P.; Fleisher, E. B. *Inorg. Chem.* **1970**, *9*, 1757.

(28) Hibbert, F.; Hunte, K. P. P. *J. Chem. Soc., Perkin Trans. 2* **1977**, 1624.

(29) Karaman, R.; Bruice, T. C. *Inorg. Chem.* **1992**, *31*, 2455.

(30) Pasternack, R. F.; Sutin, N.; Turner, D. H. *J. Am. Chem. Soc.* **1976**, *98*, 1908.

(31) Rau, W. G.; Longo, F. R. *Inorg. Chem.* **1977**, *16*, 1372.

(32) Stone, A.; Fleischer, E. B. *J. Am. Chem. Soc.* **1968**, *90*, 2735.

(33) Walter, R. I. *J. Am. Chem. Soc.* **1953**, *75*, 3860.

(34) Honda, T.; Kojima, T.; Fukuzumi, S. *Chem. Commun.* **2009**, 4994.

(35) De Luca, G.; Romeo, A.; Scolaro, L. M.; Ricciardi, G.; Rosa, A. *Inorg. Chem.* **2007**, *46*, 5979.

(36) Thyagarajan, S.; Leiding, T.; Årsköld, S. P.; Cheprakov, A. V.; Vinogradov, S. A. *Inorg. Chem.* **2010**, *49*, 9909.

(37) Almarsson, O.; Blasko, A.; Bruice, T. C. *Tetrahedron* **1993**, *49*, 10239.

(38) Hirayama, N.; Takenaka, A.; Sasada, Y.; Watanabe, E.-I.; Ogoshi, H.; Yoshida, Z.-I. *J. Chem. Soc., Chem. Commun.* **1974**, 330.

(39) Gunter, M. J.; Robinson, B. C. *Aust. J. Chem.* **1989**, *42*, 1897.

(40) Hatay, I.; Su, B.; Méndez, M. A.; Corminboeuf, C.; Khoury, T.; Gros, C. P.; Bourdillon, M.; Meyer, M.; Barbe, J.-M.; Ersoz, M.; Záliš, S.; Samec, Z.; Girault, H. H. *J. Am. Chem. Soc.* **2010**, *132*, 13733.

(41) Chirvony, V. S.; van Hoek, A.; Galievsky, V. A.; Sazanovich, I. V.; Schaafsma, T. J.; Holten, D. *J. Phys. Chem. B* **2000**, *104*, 9909.
(42) Vitasovic, M.; Gouterman, M.; Linschitz, H. *J. Porphyrins Phthalocyanines* **2001**, *5*, 191.
(43) Ransdell, R. A.; Wamser, C. C. *J. Phys. Chem.* **1992**, *96*, 10572.
(44) Gouterman, M.; Wagniere, G. H.; Snyder, L. C. *J. Mol. Spectrosc.* **1963**, *11*, 108.
(45) Adler, A. D.; Longo, F. R.; Finarelli, J. D.; Goldmacher, J.; Assour, J.; Korsakoff, L. *J. Org. Chem.* **1967**, *32*, 476.
(46) Walter, M. G.; Wamser, C. C.; Ruwitch, J.; Zhao, Y.; Braden, D.; Stevens, M.; Denman, A.; Pi, R.; Rudine, A.; Pessiki, P. J. *J. Porphyrins Phthalocyanines* **2007**, *11*, 601.

dx.doi.org/10.1021/jo400742f | *J. Org. Chem.* 2013, 78, 6040−6049